# Transferred hyperfine interactions for $Yb^{3+}$ ions in $CsCaF_3$ and $Cs_2NaYF_6$ single crystals: Experimental and *ab initio* study

M. L. Falin,[1] O. A. Anikeenok,[2] V. A. Latypov,[1] N. M. Khaidukov,[3] F. Callens,[4] H. Vrielinck,[4] and A. Hoefstaetter[5]
[1]*Zavoisky Physical-Technical Institute, 420029 Kazan, Russia*
[2]*Kazan State University, 420008 Kazan, Russia*
[3]*Institute of General and Inorganic Chemistry, 117907 Moscow, Russia*
[4]*Department of Solid State Sciences, Ghent University, Krijgslaan 281-S1, B-9000 Ghent, Belgium*
[5]*I. Physics Institute, JLU Giessen, Heinrich-Buff-Ring 16, 35392 Giessen, Germany*
(Received 28 August 2009; published 13 November 2009)

The results of an electron-nuclear double resonance study of the cubic paramagnetic $Yb^{3+}$ center in $Cs_2NaYF_6$ and $CsCaF_3$ single crystals are presented. The values and signs of the transferred hyperfine interaction (THFI) parameters for several neighboring shells are determined. It is found that the relevant parameters for the two studied matrices differ, in spite of the fact that the nearest environment of the rare earth ion is nearly identical. A first-principles theoretical analysis is performed for the THFI parameters of the first coordination shell of $F^-$ ions. Several mechanisms of metal ion-ligand coupling are considered and it is found that one of them, ligand polarization, explains the difference observed for the THFI parameters in $Cs_2NaYF_6$ and $CsCaF_3$.

DOI: 10.1103/PhysRevB.80.174110 PACS number(s): 76.70.Dx, 76.30.Kg, 71.70.Ch, 71.70.Ej

## I. INTRODUCTION

Up to now first-principles calculations of ligand hyperfine interaction parameters for paramagnetic impurity cations [transferred hyperfine interaction (THFI)] were mainly performed for ions with a nonfilled $3d$ shell by the molecular orbital method (MO-LCAO) in the approximation of a strong crystal field.[1,2] In case of an intermediate crystal field, when the free ion terms present a good zero order approximation, the Heitler-London method is more adequate. In Ref. 1 it was shown as well that taking into account covalency effects in the MO-LCAO method is equivalent to taking into account the interaction of different configurations due to the transfer of an electron from one of the ligands to the metal ion in the Heitler-London method. These ideas were developed further in Ref. 3 and were called the method of configuration interaction (CI). For the rare-earth ions (RE) the eigenstates of the total angular momentum $J$ are a good zero approximation and the crystal field presents only a weak perturbation. In this case the wave function of the paramagnetic impurity is the superposition of a very large number of determinants and the exact CI calculations in the coordinate representation become practically impossible. Nevertheless, several simplified variants of the CI method for RE centers are used by introducing fitting parameters or a series of approximations.[4,5] In such phenomenological models the observed physical properties of the RE complex are described sufficiently well by expressions proportional to the squares of the overlap integrals with the ligand atomic orbitals and the proportionality coefficients are treated as fitting parameters.[6,7] At present, to interpret spectroscopic data theoretically, density functional calculations are often used.[8,9] They are successfully applied to both impurity centers, e.g., in the calculation of the Stark splitting of $Mn^{2+}$ in $KMgF_3$,[10] and regular paramagnetic crystals, as, e.g., for the calculation of the hyperfine interactions in $La_2CuO_4$ in a cluster approximation.[11] However, in spite of a large number of papers claiming that they deal with first-principles calculations, to the best of our knowledge, there are no papers on the calculation of THFI parameters for impurity RE centers. At the same time, in the case of a RE when the ion wave functions are a good zero approximation and the metal-ligand overlap integrals are sufficiently small, it would be natural to treat this problem from a perturbation theory point of view.

As noted above, the CI solution of this problem in the coordinate representation is practically impossible because of the nonorthogonality of the orbitals of the impurity RE centers. Therefore it was natural to use the secondary-quantization method to solve this problem. In Refs. 12 and 13 the secondary-quantization method is developed on the basis of partially nonorthogonal orbitals. In these papers the dual basis is introduced. As a result, the one-particle and two-particle operators become non-Hermitian in this representation. The quantum mechanical averaging of these operators in order to reduce the Hamiltonian of the impurity center to a spin Hamiltonian is impossible because all operators herein, used to describe the experiment, are Hermitian.

Thus, the problem arises of building Hermitian operators in the secondary-quantization representation with a basis of partially nonorthogonal orbitals. Some progress in this direction was achieved in Refs. 14 and 15. However, the form of the operator was determined only with an accuracy up to the squares of the overlap integrals of the orbitals. As a consequence, the contribution of the nonorthogonality effects higher than of second order remained unclear. At the same time, the advantage of the approach proposed in Refs. 14 and 15 is that the quantum numbers of the creation and annihilation operators are the quantum numbers of the ion orbitals, allowing one to use the well-developed technique of irreducible tensor operators and secondary quantization in atomic spectroscopy.[16]

In Refs. 17–19, the main processes resulting in the appearance of hyperfine fields on the ligand nuclei in the RE impurity centers were determined by perturbation theory in

 

the framework of Refs. 14 and 15. However, the amplitudes of the electron transfer were treated as fitting parameters with their order determined by the relevant overlap integrals. This is justified in agreement with numerous results on the theory of iron-group paramagnetic impurity centers. In Refs. 20 and 21, an expression was obtained for an arbitrary operator in the orthonormalized multiparticle basis in the secondary-quantization representation with a basis of partially non-orthogonal orbitals with the creation and annihilation operators satisfying the conventional Fermi relations.

In the present paper, using the results of Refs. 20 and 21, the operators are obtained that account for the contributions to the THFI parameters from the transition of an electron to the metal ion valence shell arising in the third order of perturbation due to electron-hole interaction and to interaction of the electron transferred to the empty shell with the valence shell electrons. In contrast to Refs. 17–19, the possibility to exactly take into account the nonorthogonality effects in the considered orders of perturbation allows one to pass from the semiempirical scheme of electron transition to the construction of all possible diagrams corresponding to the considered process. In turn, these diagrams allow one to easily find the corresponding operators.

Experimentally, THFI was studied by means of electron-nuclear double resonance (ENDOR) on impurity $Yb^{3+}$ centers with cubic symmetry ($T_c$) in the cubic elpasolite ($Cs_2NaYF_6$) and perovskite ($CsCaF_3$) type single crystals. These crystals are promising materials for applications as laser media or storage phosphors and are convenient model systems to study the optical and magnetic properties of RE impurity centers and their theoretical interpretation. These single crystals are chosen because the $Y^{3+}$, $Ca^{2+}$, and $Cs^+$ cations in them have practically the same nearest environment and the interionic distances, e.g., between $Y^{3+}$ ($Ca^{2+}$) and $F^-$ [$R_{Ca^{2+}\text{-}F^-}=2.262$ Å and $R_{Y^{3+}\text{-}F^-}=2.264$ Å for $CsCaF_3$ (Ref. 22) and $Cs_2NaYF_6$ (Ref. 23), respectively], are practically identical. Nonetheless, they have different mechanisms of cation substitution by the trivalent RE, which, in turn, may influence the optical and magnetic parameters. For example, in the optical measurements of the cubic $Yb^{3+}$ center in these crystals it was observed that the crystal field parameters differ strongly.[24] Apparently, one should expect a similar situation for the THFI parameters. This creates a good model situation for testing the theory. THFI for the cubic $Yb^{3+}$ center in $Cs_2NaYF_6$ was studied by ENDOR in Ref. 25. However, it should be noted that in Ref. 25 the signs of the interaction parameters with the nearest $F^-$ shell are not reliable because they are in contradiction with the results in similar octahedral surroundings.[26] The information about the signs plays a key role in the understanding of the THFI nature. Therefore, the present work contains an additional experimental study of the THFI for this RE center.

The remainder of this paper is organized as follows. In the second section the results of the experimental study are presented. In the third section the expressions are derived for calculating the amplitudes of electron transition to a central ion with one hole in an otherwise filled shell ($4f^{13}$ configuration). The electron transition amplitudes from the ligand to the $4f$ and $5d$ shells of the central ion are calculated from first principles. The $5s$, $5p$, $4f$, and $5d$ orbitals of the central ion and $2s$ and $2p$ ligand orbitals of the free ions are chosen as basis set. Finally, the experimental results are theoretically interpreted in the fourth section.

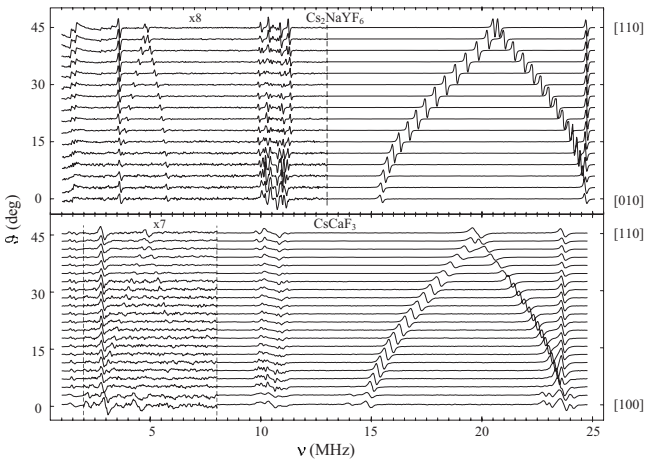


FIG. 1. Experimental angular dependence of the ENDOR spectra of the cubic $Yb^{3+}$ in $CsCaF_3$ and $Cs_2NaYF_6$ with the magnetic field H rotated in the (001) plane. 0°—[100] and 45°—[110].

## II. EXPERIMENTAL RESULTS

$CsCaF_3:Yb^{3+}$ single crystals were grown by the Bridgman-Stockbarger method in graphite crucibles in a fluorine atmosphere by adding 1.5 mol % of $YbF_3$ to the melt. The resulting concentration of $Yb^{3+}$ in the sample was approximately 0.01%. $Cs_2NaYF_6$ single crystals doped with 0.01, 0.1, 1.0, and 10.0 at. % $Yb^{3+}$ were synthesized by the chemical reaction of alkali fluoride aqueous solutions with mixtures of $Yb_2O_3$ and $Y_2O_3$ at a temperature of 750 K and pressures of 100–150 MPa. EPR and ENDOR experiments were carried out on modified *X*-band ERS-231,[27] a Bruker ESP300E *X* band, and Bruker Elexsys E500 *Q*-band spectrometers at $T=4.2-10$ K.

The analysis of the EPR spectra showed that $Yb^{3+}$ ions form several paramagnetic centers (PCs) in $CsCaF_3$ with different symmetries: cubic ($T_c$), tetragonal, and trigonal. In $Cs_2NaYF_6$, the $Yb^{3+}$ ions form one PC, $T_c$. The THFI were only studied for the $T_c$ centers in both crystals. In order to accurately identify the ENDOR lines as belonging to definite $F^-$ and $Cs^+$ ions and to determine the THFI parameters, their angular dependences were recorded on the even $Yb^{3+}$ isotope while rotating the magnetic field $H$ in a {001} plane (Fig. 1). The interpretation of the ENDOR spectra showed that at the formation of $T_c$ in $CsCaF_3$, the $Yb^{3+}$ ions substitute $Ca^{2+}$ (aliovalent substitution), i.e., the excess positive charge is compensated nonlocally, and in $Cs_2NaYF_6$ they substitute $Y^{3+}$ isovalently. Figure 2 shows the fragments of the crystal structures of the two matrices studied. The positions of the $Yb^{3+}$ impurity ions are shown. $Yb^{3+}$ ions in a perfect octahedral crystal field have the $\Gamma_6$ Kramers doublet as ground state. The ENDOR spectra are described by the standard spin Hamiltonian.[27] The obtained THFI parameters are given in Table I, where $T_\parallel$ and $T_\perp$ are the principal values of the THFI

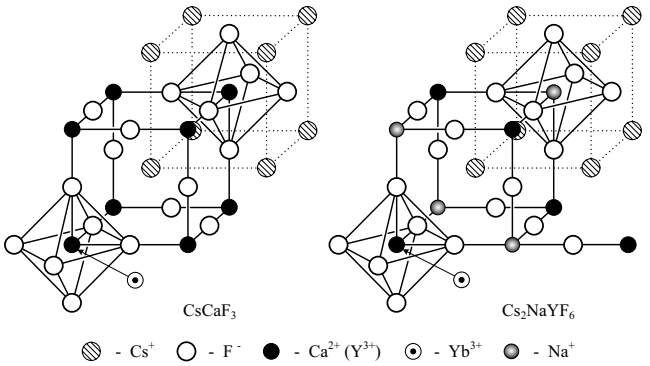


FIG. 2. Fragments of the crystal lattices of $CsCaF_3$ and $Cs_2NaYF_6$.

tensor, and $A_s=(T_\parallel+2T_\perp)/3$ and $A_p=(T_\parallel-T_\perp)/3$ are their isotropic and anisotropic parts, respectively. For comparison, the data for $Yb^{3+}$ in $KMgF_3$ and $KZnF_3$ (Ref. 26) are given in Table I as well. The sign of the $g$ factors is determined theoretically.[28] To determine the signs of the THFI parameters, the method developed in Ref. 29 was used. Figure 3 shows the ENDOR frequencies of the fluorine transitions of the first coordination shell observed on the different $Yb^{3+}$ isotopes in $Cs_2NaYF_6$, compared with those calculated for different signs of the THFI parameters. Experimental and theoretical points practically coincide with the results of the present work. Table I shows that the THFI parameters for $Cs_2NaYF_6:Yb^{3+}$ determined in this paper coincide with data of Ref. 25 but have opposite signs. It was established that the THFI parameters of $Yb^{3+}$ for fluorine elpasolites and perovskites have the same sign, i.e., the dominant mechanisms of the rare-earth ion–ligand coupling in the two fluoride compounds are similar. It should be noted that the method[29]

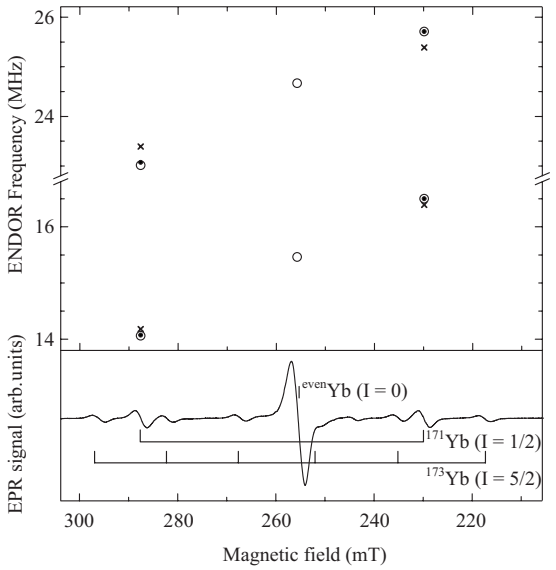


FIG. 3. Dependence of the first $^{19}F$ shell ENDOR frequencies on the magnetic resonance field for $^{even}Yb^{3+}$ and $^{171}Yb^{3+}$ isotopes in $Cs_2NaYF_6$. ○—experiment, ●—calculated with parameters given in this paper, and ×—calculated with parameters of Ref. 25. The EPR spectrum of $T_c$ $Yb^{3+}$ is shown at the bottom. The hyperfine structure lines of the $Yb^{3+}$ isotopes are shown as well.

allowed us to determine not only the signs of the THFI parameters but also the signs of the hyperfine interaction constant ($A$) for the $^{171}Yb$ and $^{173}Yb$ isotopes in $Cs_2NaYF_6$ ($^{171}A=-2057$ MHz and $^{173}A=567$ MHz) and specify them for the $A$ values in $CsCaF_3$ ($^{171}A<0$ and $^{173}A>0$) given in Ref. 30. Figure 4 shows the experimental and theoretical angular dependences plotted on the basis of data from Table I. It is seen that the experimental dependences are described

TABLE I. Experimental THFI parameters (in MHz) of $Yb^{3+}$ with fluorine and cesium ions. $a_o$ is the crystal lattice constant (in Å). $R$ is the distance between $Yb^{3+}$ and the corresponding ligand in the undistorted crystal lattice. $A_d$ is the parameter of the dipole-dipole interaction ($g\beta g_n\beta_n/R^3$).

| | $g$ factor | Ligand ion | Coordination ligand shell | $R$ (Å) | $T_\parallel$ | $T_\perp$ | $A_s$ | $A_p$ | $A_d$ | |
|---|---|---|---|---|---|---|---|---|---|---|
| $CsCaF_3$ | (−)2.591 | F | I | 2.262 | 8.651 | 26.540 | 20.577(10) | −5.963(10) | −8.289 | |
| $a_o=4.523$[a] | | | II | 5.058 | −1.513 | 0.730 | −0.025(10) | −0.755(10) | −0.741 | |
| | | Cs | I | 3.917 | 0.446 | 0.223 | 0 | −0.214(10) | −0.223 | |
| $Cs_2NaYF_6$ | (−)2.588(5) | F | I | 2.264 | 9.695 | 28.319 | 22.111(10) | −6.208(10) | −8.268 | |
| $a_o=9.066$[b] | | | II | 5.068 | −1.491 | 0.761 | 0.015(10) | −0.746(10) | −0.740 | |
| | | Cs | I | 3.926 | −0.442 | 0.221 | 0 | −0.221(10) | −0.222 | |
| $Cs_2NaYF_6$ | (−)2.581 | F | I | | | | −22.07 | 6.198 | 8.19 | [c] |
| | | Cs | I | | | | −0.006 | 0.239 | 0.221 | |
| $KZnF_3$ | (−)2.582 | F | I | 2.020 | 11.415 | 29.211 | 23.065 | −5.965 | −11.645 | [d] |
| $a_o=4.040$ | | | | | | | | | | |
| $KMgF_3$ | (−)2.584 | F | I | 1.987 | 11.135 | 29.03 | 23.279 | −5.932 | −12.283 | |
| $a_o=3.973$ | | | | | | | | | | |

[a]Reference 5.
[b]Reference 6.
[c]Reference 25.
[d]Reference 26.

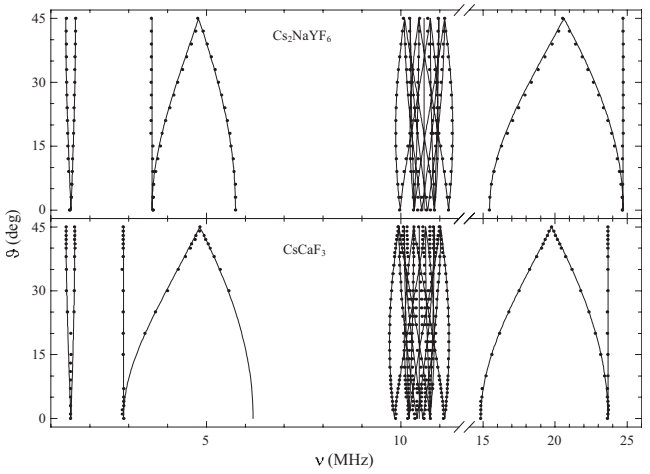


FIG. 4. Experimental and theoretical angular dependences of the ENDOR lines in the (001) plane. ●—experiment and——theory with the THFI parameters from Table I. 0°—[100] and 45°—[110].

very well. The THFI parameters for the fluorine ions of the second coordination sphere of F and Cs practically coincide with the data calculated according to the dipole model. This indicates that the relaxation of the crystal lattices in the vicinity of $Yb^{3+}$ is small and the coincidence of the interionic distances $R_{Yb^{3+}\text{-}F^-}$ in both crystals. Nevertheless, analogous to the optical studies in Ref. 24, it is observed that the THFI parameters $A_s$ and $A_p$ for the first $F^-$ coordination sphere in the studied crystals differ strongly. It should be noted as well that data for $Cs_2NaYF_6$ do not fit the general dependence observed for these parameters on the $Yb^{3+}$-$F^-$ distance (calculated for the undistorted crystal lattices) in the homologous series of cubic perovskite type fluorides (Fig. 5).

## III. THEORY

Let us denote the one-particle operator $h$ as a sum of the kinetic energy of electron, electron-nuclear Coulomb interaction, and Coulomb interaction of electron with the crystal lattice and the two-particle operator $u$ as the Coulomb interaction of electrons. In Ref. 20 it was shown that an arbitrary operator $H$ being a sum of $h$ and $u$ in a basis set of partially nonorthogonal orbitals may be expressed in the form of an operator series of $H_\Psi$. In this case, under the assumption of the existence of the $(I+S)^{-1}$ matrix with $I$ being a unit operator and $S$ being the overlap matrix for one-electron orbitals, the effects of nonorthogonality are exactly taken into account in each term of the above series. Then according to Ref. 20,

$$H_\Psi = \sum_{n=0}^{\infty} c_n [Q,\bar{H}]^{(2n)}, \quad c_n = \frac{E_{2n}}{2^{2n}(2n)!}, \tag{1}$$

where $H_\Psi$ is determined on the functions

$$|\{\xi\}\rangle = \prod_{\xi} a_\xi^+ |0\rangle,$$

$a_\xi^+$ $(a_\xi)$ is the creation (annihilation) operators for electrons in the ion orbitals. In contrast to Refs. 12 and 13, where the anticommutator of the creation and annihilation operators of the ion orbitals is equal to the corresponding overlap integral, here $a_\xi^+$ $(a_\xi)$ satisfy the conventional relations for Fermi operators, i.e.,

$$a_\xi a_{\xi'} + a_{\xi'} a_\xi = a_\xi^+ a_{\xi'}^+ + a_{\xi'}^+ a_\xi^+ = 0, \quad a_{\xi'} a_\xi^+ + a_\xi^+ a_{\xi'} = \delta_{\xi\xi'}$$

Note that the particle number operator number in our approach is[21]

$$N_\Psi = \sum a_\xi^+ a_\xi$$

Interestingly, careful consideration showed that $E_{2n}$ in Eq. (1) are Euler numbers ($E_0=1$, $E_2=-1$, $E_4=5$, $E_6=-61$, $E_8=1385$, $E_{10}=-50521$, etc.). It follows from the properties of the series with $c_n$ coefficients that, in case the matrix elements of the $[Q,\bar{H}]^{(2n)}$ operators are bounded, they are convergent,[31]

$$\bar{H} = \sum a_\xi^+ a_{\xi'} \langle \xi|\bar{h}|\xi'\rangle + \frac{1}{2} \sum a_\xi^+ a_\eta^+ a_{\eta'} a_{\xi'} \langle \xi\eta|\bar{u}|\xi'\,\eta'\rangle,$$

$$\langle \xi|(I+S)^{-1}|\theta\rangle \equiv \langle \xi||\theta\rangle,$$

$$\langle \xi|(I+S)^{-1}|\theta\rangle\langle \eta|(I+S)^{-1}|\varsigma\rangle \equiv \langle \xi\eta||\theta\varsigma\rangle,$$

$$\langle \xi|\bar{h}|\xi'\rangle = \frac{1}{2} \sum \langle \xi||\theta\rangle\langle\theta|h|\xi'\rangle + \frac{1}{2} \sum \langle \xi|h|\theta\rangle\langle\theta||\xi'\rangle,$$

$$\langle \xi\eta|\bar{u}|\xi'\,\eta'\rangle = \frac{1}{2} \sum \langle \xi\eta||\theta\varsigma\rangle\langle\theta\varsigma|u|\xi'\,\eta'\rangle + \frac{1}{2} \sum \langle \xi\eta|u|\theta\varsigma\rangle\langle\theta\varsigma||\xi'\,\eta'\rangle,$$

where the operator $Q=\Sigma a_\xi^+ a_{\xi'} \langle \xi|q|\xi'\rangle$, $q=\ln(I+S)$, and $h$ and $u$ are the one-particle and two-particle operators, respectively,

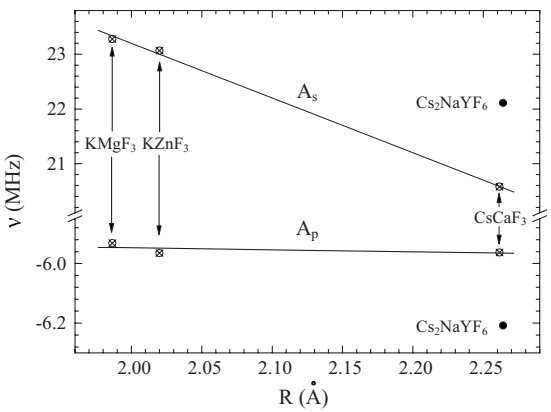


FIG. 5. Dependence of the THFI parameters $A_s$ and $A_p$ on the distance between $Yb^{3+}$ and the fluorine ion of the nearest environment in perovskite-type crystals and $Cs_2NaYF_6$.

$$[Q,\bar{H}]^{(n)} \equiv [Q,[Q,\cdots[Q,\bar{H}]\cdots]], \tag{2}$$

where $[Q,\bar{H}]$ is the commutator and the expression in the right-hand side of Eq. (2) denotes $n$ commutators.

Let us consider the operator $q=\ln(I+S)$. Its matrix elements in the case of a convergent logarithmic series may be calculated from

$$\ln(I+S) = S - \frac{S^2}{2} + \frac{S^3}{3} - \cdots. \tag{3}$$

It is possible to formally present the left-hand side of equality (3) as an integral

$$\ln(I+S) = \int_0^1 (I+\alpha S)^{-1} d\alpha \approx S\sum_{i=1}^{N} (I+\alpha_i S)^{-1}\Delta\alpha, \tag{4}$$

where $(I+\alpha_i S)^{-1}$ is the matrix reciprocal to $(I+\alpha_i S)$ and $\alpha_i = i/N$. However, the expression on the right from the sign of approximate equality is an integral sum of this integral. It exists always when the matrix $(I+S)^{-1}$ exists. It is easy to check by direct calculation that if series (3) is convergent, the integral sum in Eq. (4) already at $N=10^6$ and $\Delta\alpha=10^{-6}$ coincides with Eq. (3) with high accuracy. Calculations show that if series (3) is divergent, the matrix calculated according to Eq. (4) exists. For overlap integrals which are sufficiently small, the corresponding matrix elements (4) have the same sign and order of magnitude as the values of these integrals. Therefore, the matrix elements of the operator $q=\ln(I+S)$ will further on be understood in the sense of equality (4). Thus, in general the value of the overlap integrals can be arbitrary.

### A. Operator of transferred hyperfine interaction

To derive the operator of the hyperfine interaction on the ligand, we use the formalism of perturbation theory for degenerate states as considered in Ref. 32. The $\bar{H}_0$ operator used in the present paper is defined according to Ref. 17. Then the operator of the transferred hyperfine interaction $V$, acting in the space of the low-lying quasidegenerate states of the Hamiltonian $\bar{H}_0$ and written down with accuracy to the third-order terms in the metal-to-ligand transition energy, is as follows:

$$V = \bar{V} - \frac{1}{8}[Q,\bar{V}]^{(2)} + [\bar{V},(F_1+F_2)] - F_1\bar{V}F_1 - F_1\bar{V}F_2 - F_2\bar{V}F_1,$$

$$F_{1ml} = -\frac{\bar{H}_{ml}}{\Delta_{ml}}, \quad \Delta_{ml} = E_m - E_l$$

where $E_m$ and $E_l$ are the zero-order energies of the low-lying quasidegenerate states and of the excited states, respectively. $\bar{H}_{ml}$, $\bar{H}_{mm'}$, and $\bar{H}_{l'l}$ are matrix elements of the Hamiltonian operators considered as a perturbation,

$$F_{2ml} = \sum_{m'} \frac{\bar{H}_{mm'}\bar{H}_{m'l}}{\Delta_{ml}\Delta_{m'l}} - \sum_{l'} \frac{\bar{H}_{ml'}\bar{H}_{l'l}}{\Delta_{ml}\Delta_{ml'}}, \quad F_{mm'} = F_{ll'} = 0.$$

Let us now in particular consider processes leading to the appearance of the hyperfine fields on the ligand nuclei. The contribution from the electron transition from a ligand orbital to the partially filled central ion shell is found as follows. The operator $V_1$ corresponding to these processes is written in the secondary-quantization presentation.[16] Then, by restricting to second-order perturbation terms, we get

$$V_1 = \sum a_\xi^+ a_{\xi'}\left[\frac{1}{4}\langle\xi|q|\varsigma\rangle\langle\theta|q|\xi'\rangle - \frac{1}{2}\bar{\gamma}_{\xi\varsigma}\langle\theta||\xi'\rangle - \frac{1}{2}\langle\xi||\varsigma\rangle\bar{\gamma}_{\theta\xi'} + \bar{\gamma}_{\xi\varsigma}\bar{\gamma}_{\theta\xi'}\right]\langle\varsigma|\nu|\theta\rangle, \tag{5}$$

where $\nu$ is the hyperfine interaction operator, and $\xi$, $\xi'$ and $\theta$, $\zeta'$ are quantum numbers of the central ion and ligand orbitals, respectively,

$$\bar{\gamma}_{\xi\varsigma} = -\frac{\langle\xi|G|\varsigma\rangle}{|\Delta_{\{\xi\},\{\varsigma\}}|},$$

$\langle\xi|G|\varsigma\rangle$ is the amplitude of the electron transition from the ligand to the central ion, $\varsigma$ is the ligand orbital, $\xi$ is the central ion orbital, $|\Delta_{\{\xi\},\{\varsigma\}}|$ is the transition energy from ground to excited state. Formula (1) shows that the corrections to Eq. (5) from the fourth-order commutators will be fourth- and higher-order corrections on the metal-ligand overlap area. Moreover, the ratio of the coefficients of the third and second terms in Eq. (1) is 0.104 17. Therefore in this paper these corrections are supposed to be small and will be neglected.

In Eq. (5), nonorthogonality effects are taken into account exactly, under the supposition that the matrix $(I+S)^{-1}$ exists. For the further calculations it is therefore necessary to derive expressions for the electron transition amplitudes to the partially filled shell. Within the present approach expressions for the electron transition amplitudes to the higher empty shells were obtained and discussed in Ref. 33. In the general case, the operator of electron transition from one ion to another is a two-particle operator. However, following Ref. 33 it is easy to show that for transition to a shell having one electron less than the completely filled shell (configurations $3d^9$, $4f^{13}$, etc.), it reduces to a one-particle operator,

$$G\langle f|b\rangle = \sum a_\xi^+ a_\varsigma \langle\xi|G|\varsigma\rangle,$$

where $\varsigma$ is the orbital of ligand $b$, and $\xi$ is the central ion orbital.

$$2\langle\xi|G|\varsigma\rangle = \langle\xi||\varsigma\rangle\Bigg[\varepsilon_{\xi}^{q_e-1} + \sum_{\dot\eta_e}\langle\xi\dot\eta_e|u(1-P)|\xi\dot\eta_e\rangle(\langle\dot\eta_e||\dot\eta_e\rangle - 1) + h_M^{\xi} + \varepsilon_{\varsigma}^{q_b} + \sum_{\dot\eta_b}\langle\varsigma\dot\eta_b|u(1-P)|\varsigma\dot\eta_b\rangle(\langle\dot\eta_b||\dot\eta_b\rangle - 1) + h_M^{\varsigma}$$
$$- \langle\varsigma|\frac{n_e+m_e}{|\boldsymbol{r}-\boldsymbol{R}_e|}|\varsigma\rangle + \sum_{\dot\eta_e\neq\xi}\langle\varsigma\dot\eta_e|u(1-P)|\varsigma\dot\eta_e\rangle\langle\dot\eta_e||\dot\eta_e\rangle - \langle\xi|\frac{n_b+m_b}{|\boldsymbol{r}-\boldsymbol{R}_b|}|\xi\rangle + \sum_{\dot\eta_b\neq\varsigma}\langle\xi\dot\eta_b|u(1-P)|\xi\dot\eta_b\rangle\langle\dot\eta_b||\dot\eta_b\rangle\Bigg] + (\langle\xi||\xi\rangle$$
$$+ \langle\varsigma||\varsigma\rangle)\Bigg[\langle\xi|h_k|\varsigma\rangle - \langle\xi|\frac{n_e+m_e}{|\boldsymbol{r}-\boldsymbol{R}_e|}|\varsigma\rangle + \sum_{\dot\eta_e}\langle\xi\dot\eta_e|u(1-P)|\varsigma\dot\eta_e\rangle\langle\dot\eta_e||\dot\eta_e\rangle - \langle\xi|\frac{n_b+m_b}{|\boldsymbol{r}-\boldsymbol{R}_b|}|\varsigma\rangle + \sum_{\dot\eta_b}\langle\xi\dot\eta_b|u(1-P)|\varsigma\dot\eta_b\rangle\langle\dot\eta_b||\dot\eta_b\rangle\Bigg], \tag{6}$$

where all quantities referring to the central ion are denoted with an index $e$, those referring to the ligand with an index $b$, $u$ is the Coulomb interaction of electrons, and $P$ is the permutation operator. The summation over $\dot\eta_e$ includes all orbitals of the filled shells in the ground configuration and all valence shell orbitals for the central ion. Summation over $\dot\eta_b$ runs over all ligand orbitals in the ground configuration. The $\varepsilon_{\xi}^{q_e-1}$ and $\varepsilon_{\varsigma}^{q_b}$ values are Hartree-Fock energies of the electron on the orbital $\xi$ of the central ion and on the ligand orbital $\varsigma$, respectively, as determined for free ions; $h_k$ is the kinetic energy operator; $h_M^{\xi}$ and $h_M^{\varsigma}$ are the Madelung energies of the electron on the central ion and ligand, respectively. $h_l=|\boldsymbol{r}-\boldsymbol{R}_l|^{-1}$, $l=e$, $b$; and $n_e+m_e$ and $n_b+m_b$ are the sum of the number of electrons and shifts from the ion charge in the pure crystal in the ground configuration on the central ion and ligand, respectively.

Let us consider the following third-order process. The electron is transferred from the ligand to the valence shell of the central ion. Then the valence shell electron is transferred to one of the higher lying orbitals by the electrostatic field of the hole occurring on the ligand (the electron-hole interaction) and returns. The $V_2$ operator taking into account the contributions of such processes to the constants of the THFI was obtained in Ref. 18. The covalency parameters were considered as the fitting parameters and the nonorthogonality effects were taken into account by assuming $(I+S)^{-1}\approx I-S$. By using the present approach, for the operator $V_2$ we obtain

$$V_2 = \sum a_{\xi}^{+}a_{\xi'}\frac{\langle\xi|h_{eh}|\varphi\rangle}{|\Delta_{\xi\varsigma}|}\Bigg[\frac{1}{4}\langle\varphi||\varsigma\rangle\langle\theta||\xi'\rangle - \frac{1}{2}\langle\varphi||\varsigma\rangle\bar\gamma_{\theta\xi'}$$
$$+ \frac{1}{2}\bar\gamma_{\varphi\varsigma}\langle\theta||\xi'\rangle - \left(1+\frac{|\Delta_{\xi\varsigma}|}{|\Delta_{\varphi\theta}|}\right)\bar\gamma_{\varphi\varsigma}\bar\gamma_{\theta\xi'}\Bigg]\langle\varsigma|\nu|\theta\rangle + \text{H.c.} \tag{7}$$

where $\xi$ and $\xi'$ are the quantum numbers of the valence shell orbitals, $\varphi$ are the quantum numbers of the orbitals of the higher-lying empty shells, $\theta$ and $\varsigma$ are the quantum numbers of the ligand orbitals, and $h_{eh}$ is the operator of the electron-hole interaction. Note that on the basis of Eq. (1) the form of operator (7) can be easily determined by using the diagram method. If the 6a and 6b diagrams in Fig. 6 corresponding to the fourth term in square brackets in Eq. (7) are called the forming ones, then the 6ab1, 6ab2, and 6ab3 diagrams are obtained by including the matrix elements of the $(I+S)^{-1}$ matrix in it. The diagrams Hermitian conjugated to the 6a, 6ab1, 6ab2, and 6ab3 refer to the same situation. The 6b diagram is not Hermitian conjugated to the 6a diagram. At the same time, the introduction of the matrix elements of $(I+S)^{-1}$ in this diagram does not result in new diagrams since they are Hermitian conjugated to the 6ab1, 6ab2, and 6ab3 diagrams. Thus we obtained all possible operators of the perturbation series corresponding to the process under consideration.

Next, let us consider the following process. An electron from the ligand goes to a higher empty shell of the central ion. As a result of the Coulomb exchange interaction, contributions to the hyperfine field on the ligand from transitions of the electron with spin up differ from those with down. The operator $V_3$, taking into account contributions to the transferred hyperfine constant from such processes in the framework of a semiempirical approach, is given in Ref. 17. By using the present approach, for $V_3$ we obtain

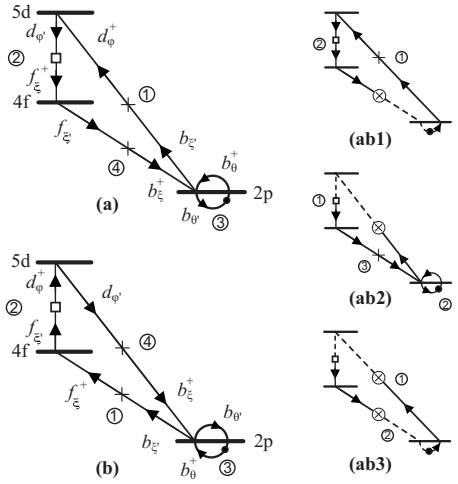


FIG. 6. Processes of the electron transfer to the 5*d* shell, where $G_{\mathrm{p,d}}$ is the amplitude of electron transition from the ligand 2*p* shells to the 4*f* and 5*d* shells of the REI, $h_{eh}$ is the operator of the electron-hole interaction, $\nu$ is the operator of the hyperfine interaction, $f_{\xi'}{}^{+}$, and $f_{\xi'}$ are the creation and annihilation operators of the 4*f*-shell electrons, $d_{\varphi}{}^{+}$ and $d_{\varphi}$ are the creation and annihilation operators of the 4*d*-shell electrons $b^{+}$ and $b$ are the creation and annihilation operators of the ligand 2*s* and 2*p* shell electrons, and 1–4—sequence of the electron transitions (see text for details).

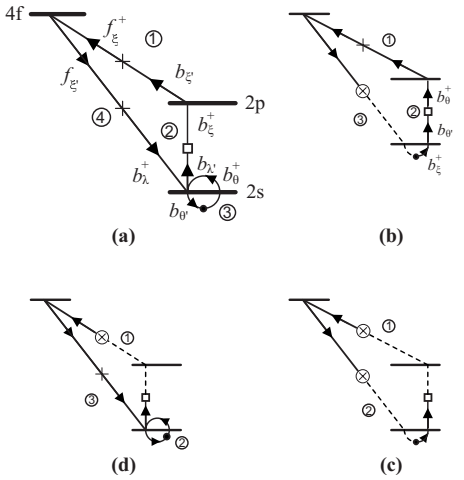


FIG. 7. Diagram of the ligand polarization, where $G_{s,p}$ is the amplitude of electron transition for the ligand $2s$ and $2p$ shells to the REI $4f$ shell, $h_{eh}$ is the operator of the electron-hole interaction, $\nu$ is the operator of the hyperfine interaction, $f_{\xi'}{}^{+}$, and $f_{\xi'}$ are the creation and annihilation operators of the $4f$-shell electrons, $b^{+}$ and $b$ are the creation and annihilation operators of the ligand $2s$ and $2p$-shell electrons, and 1–4—sequence of the electron transitions (see text for details).

$$V_3 = \sum a_{\xi}^{+} a_{\xi'} \frac{\langle \xi\varphi | u(1-P) | \xi'\varphi' \rangle}{|\Delta_{\varphi\varsigma}|} \left[ \bar{\gamma}_{\varphi'\varsigma} \bar{\gamma}_{\theta\varphi} - \frac{1}{4} \langle \varphi' || \varsigma \rangle \langle \theta || \varphi \rangle \right] \times \langle \varsigma | \nu | \theta \rangle + \text{H.c.}$$

where $\xi$ and $\xi'$ are the quantum numbers of the valence shell orbitals, $\varphi$ and $\varphi'$ are the quantum numbers of higher empty shell orbitals, $\theta$ and $\varsigma$ are quantum numbers of the ligand orbitals, and $u$ is the Coulomb interaction operator of the electrons.

Finally, let us consider another third-order process. The electron goes from the ligand to the valence shell of the central ion. Then the electron-hole interaction transfers the hole on the ligand to the other orbital and the electron returns back. This process can be considered as the ligand polarization. By using the present approach, we obtain for the operator $V_4$,

$$V_4 = \sum a_{\xi}^{+} a_{\xi'} \left[ \frac{1}{4} \langle \xi || \varsigma \rangle \langle \theta || \xi' \rangle - \frac{1}{2} \langle \xi || \varsigma \rangle \bar{\gamma}_{\theta\xi'} - \frac{1}{2} \bar{\gamma}_{\xi\varsigma} \langle \theta || \xi' \rangle + \bar{\gamma}_{\xi\varsigma} \bar{\gamma}_{\theta\xi'} \right] \frac{\langle \varsigma | h_{eh} | \lambda \rangle}{|\Delta_{\xi\lambda}|} \langle \lambda | \nu | \theta \rangle + \text{H.c.} \quad (8)$$

where $\xi$ and $\xi'$ are quantum numbers of the valence shell orbitals, $\theta$, $\varsigma$, and $\lambda$ are quantum numbers of ligand orbitals, and $h_{eh}$ is the operator of the electron-hole interaction. The form of the operator $V_4$ can be determined with the diagrams in Fig. 7, the same as that of the $V_2$ operator. Figures 7(a)–7(d) determines the fourth, second, first, and third terms in square brackets in Eq. (8), respectively.

It is obvious that the operator $V_4$ is the next-order correction to the operator $V_1$. Unlike $V_2$, two cases should be considered for $V_4$. If the valence of the dopant ion is one unit larger than that of the host ion, then at the electron transition from the ligand to the central ion the charge symmetry of the ligand environment is restored. The transitions at the ligand, forbidden for the host crystal, will be forbidden in the considered excited configuration as well, at least in the approximation of an electrostatic field. In the case of isovalent substitution the charge symmetry of the ligand environment is broken and the transitions forbidden for the ground configuration may become allowed.

In Ref. 19, it is proposed to take into account another type of processes resulting in the appearance of hyperfine fields on the ligand nuclei. These processes include the so-called core polarization.[16] However, to determine the relevant contributions from first principles it is necessary to calculate the electron transition amplitudes of from the ligand to the $5s$, $5p$, $6s$, and $6p$ shells of the RE ion. The transition amplitudes to the $5s$ and $5p$ shells can be calculated by perturbation theory because using the one-particle basis of the present work the $p_{5si}$ and $p_{5pi}$ matrix elements are on the order of 0.05–0.1. However the possibility to account also for the $6s$ and $6p$ orbitals correctly from the mathematical point of view, i.e., calculating the $(I+S)^{-1}$ matrix including these orbitals, requires a separate consideration. Note that the $6s$ and $6p$ orbitals are used long ago in many parametric approaches and therefore it is natural to include them in first-principles calculations. At the same time, the length of the Hartree-Fock $6s$ and $6p$ orbitals of the free trivalent ions is comparable with the distance between the ions. Hence, already in the zero approximation of their correction it is necessary to take the influence of at least the nearest environment into account, i.e., using the Hartree-Fock method for nonorthogonal orbitals.[34,35] Here this contribution was only estimated in the framework of Ref. 19.

### B. Operator matrix elements

In this section we give the numerical values of the operator matrix elements in the above expressions for $Yb^{3+}$ octahedrally surrounded by fluorine ions. Let us choose the coordinate system as follows. The RE ion is placed in the coordinate origin, the $z$ axis directed along the fourfold axis. The ligand coordinates then become $1(a,0,0)$, $2(0,a,0)$, $3(0,0,a)$, $4(-a,0,0)$, $5(0,-a,0)$, and $6(0,0,-a)$. We perform all calculations for the electron transition from ligand $6(0,0,-a)$. The true $R_{Yb^{3+}\text{-}F^{-}}$ distance in the crystals under study is not known; therefore in the calculations below the value $R_{Yb^{3+}\text{-}F^{-}}=2.20$ Å was used, being the sum of the ionic radii for $Yb^{3+}$ and $F^{-}$.[36]

We used the basis of $5s$, $5p$, and $4f$ orbitals,[37] $5d$ orbitals[38] for the central ion, and $2s$ and $2p$ ligand orbitals,[37] thus $(I+S)^{-1}$ is a $40\times40$ matrix. No analytical or numerical expressions are available for the $5d$ orbitals of $Yb^{3+}$. We assumed that Hartree-Fock orbitals of chemically related ions present a sufficiently accurate approximation.[37] The $Yb^{3+}$ $5d$ orbitals were obtained by Gaussian approximation of the numerical representation of these orbitals for $Tm^{3+}$.[38]

The elements of the $(I+S)^{-1}$ matrix and of the one-particle operators in Eq. (6), necessary for calculating the electron transition amplitudes from the $2s$- and $2p0$-ligand orbitals to the $4f0$ orbital of $Yb^{3+}$ are given in Table II,

TABLE II. Matrix elements of the $(I+S)^{-1}$ matrix and the one-particle operators (in a.u.). Here and in Tables III and IV the calculations were performed for the distance $R_{Yb^{3+}\text{-}F^-}=2.20$ Å.

| $a$ | $5s$ | $5p0$ | $5p1$ | $4f0$ | $4f1$ | $4f2$ | $4f3$ | $2s$ | $2p0$ |
|---|---|---|---|---|---|---|---|---|---|
| $\langle a\|\|a\rangle$ | 1.06154 | 1.0387 | 1.0387 | 1.00068 | 1.00036 | 1.0008 | 1.00049 | 1.04926 | 1.06558 |
| $a, b, i$ | $4f0, 2s, k$ | $4f0, 2s, e$ | $4f0, 2s, b$ | $4f0, 2p0, k$ | $4f0, 2p0, e$ | $4f0, 2p0, b$ | $4f0, 4f0, b$ | $2s, 2s, e$ | $2p0, 2p0, e$ |
| $\langle a\|h_i\|b\rangle$ | 0.00115465 | −0.00371964 | −0.00617715 | −0.00587399 | −0.0063791 | −0.00892204 | 0.24290 | 0.24051 | 0.25166 |

$$h_M^e = 0.82, \quad h_M^b = -0.43, \quad \varepsilon_{4f}^{Yb^{3+}} = -2.006,$$
$$\varepsilon_{2s}^{F^-} = -1.0744, \quad \varepsilon_{2p}^{F^-} = -0.18.$$

The value of $\varepsilon_\xi^{q_e-1}=\varepsilon_\xi^{Yb^{2+}}$ was determined using the wave functions of the trivalent $Yb^{3+}$ ion: in the zero order approximation they can be presented as $\varepsilon_\xi^{Yb^{2+}}=\varepsilon_\xi^{Yb^{3+}}+\langle\xi+,\xi-|u|\xi+,\xi-\rangle$, where $\pm$ are projections of the electron spin on the $\xi$ orbitals. This corresponds to the main assumption that the virtual processes of charge transfer may be taken into account in perturbation theory.[39] The values of the necessary two-center integrals of the Coulomb interaction between electrons are given in Table III.

Estimations of the contributions $\Sigma_{\eta_b\neq\zeta}\langle\xi\eta_b|u(1-P)|\xi\eta_b\rangle\langle\eta_b||\eta_b\rangle-\langle\xi|(n_b-1)/|(\boldsymbol{r}-\boldsymbol{R}_b)||\xi\rangle$ show that they can be neglected in the calculation of the transition amplitudes.

By substituting these numerical values into Eq. (6), the transition amplitudes are obtained as

$$\langle 4f0|G|2s\rangle \equiv G_{4fs} = 0.013\ 834 \text{ a.u.},$$
$$\langle 4f0|G|2p0\rangle \equiv G_{4f\sigma} = 0.016\ 842 \text{ a.u.}$$

The calculation of the transition amplitude from the $2p1$ orbital to the $4f1$ orbital is analogous to the calculation of that from the $2p0$ orbital to the $4f0$ orbital and its final result is given,

$$\langle 4f1|G|2p1\rangle \equiv G_{4f\pi} = -0.008\ 653 \text{ a.u.}$$

According to Ref. 18 $\Delta_{4f,2s}\approx 1.1$ a.u. and $\Delta_{4f,2p}\approx 0.27$ a.u.. Thus,

$$\bar{\gamma}_{4fs} = -0.0125, \quad \bar{\gamma}_{4f\sigma} = -0.0624, \quad \bar{\gamma}_{4f\pi} = 0.0320.$$

By using the results of Ref. 33 covalency parameters of the $5d$ shell are obtained as follows:

$$\bar{\gamma}_{5ds} = 0.132, \quad \bar{\gamma}_{5d\sigma} = 0.154, \quad \bar{\gamma}_{5d\pi} = -0.0784.$$

## IV. DISCUSSION

We now calculate the contributions of the aforementioned processes to the THFI parameters of the centers under consideration. Let us introduce the following notations:

$$q_{\xi\theta} \equiv \langle\xi|q|\theta\rangle, \quad p_{\xi\theta} \equiv \langle\xi||\theta\rangle. \tag{8'}$$

We write the quantum numbers in Eq. (8) down analogous to their form in the transition amplitudes and introduce functions to express the contributions of the considered processes. Note that, under the condition of small two-particle

TABLE III. Two-center integrals of the Coulomb interaction of electrons (in $\times 10^2$ a.u.). In the $\langle ab|u|cd\rangle$ matrix element the orbital $|a\rangle=|4f0\rangle$.

| $bcd$ | $5s, 2s, 5s$ | $5s, 5s, 2s$ | $5p0, 2s, 5p0$ | $5p0, 5p0, 2s$ | $5p1, 2s, 5p1$ |
|---|---|---|---|---|---|
| $\langle ab\|u\|cd\rangle$ | −0.359219 | −0.0138135 | −0.426358 | −0.0998833 | −0.31784 |
| $bcd$ | $4f2, 4f2, 2s$ | $4f3, 2s, 4f3,$ | $4f3, 4f3, 2s$ | $4f0, 2s, 4f0$ | $2s, 2s, 2s$ |
| $\langle ab\|u\|cd\rangle$ | 0.0151758 | −0.338201 | 0.0136855 | −0.403948 | −0.569773 |
| $bcd$ | $5s, 2p0, 5s$ | $5s, 5s, 2p0$ | $5p0, 2p0, 5p0$ | $5p0, 5p0, 2p0$ | $5p1, 2p0, 5p1$ |
| $\langle ab\|u\|cd\rangle$ | −0.605976 | −0.0278836 | −0.796907 | −0.249456 | −0.492915 |
| $bcd$ | $4f2, 2p0, 4f2$ | $4f2, 4f2, 2p0$ | $4f3, 2p0, 4f3$ | $4f3, 4f3, 2p0$ | $2p0, 2p0, 2p0$ |
| $\langle ab\|u\|cd\rangle$ | −0.602084 | 0.0666222 | −0.524371 | 0.0628218 | −0.891938 |
| $bcd$ | $5p1, 5p1, 2s$ | $4f1, 2s, 4f1$ | $4f1, 4f1, 2s$ | $4f2, 2s, 4f2$ | |
| $\langle ab\|u\|cd\rangle$ | 0.0165205 | −0.390274 | −0.0119372 | −0.361699 | |
| $bcd$ | $2p0, 2s, 2p0$ | $2p0, 2p0, 2s$ | $2p1, 2s, 2p1$ | $2p1, 2p1, 2s$ | |
| $\langle ab\|u\|cd\rangle$ | −0.584476 | −0.243708 | −0.518993 | −0.0505651 | |
| $bcd$ | $5p1, 5p1, 2p0$ | $4f0, 2p0, 4f0$ | $4f1, 2p0, 4f1$ | $4f1, 4f1, 2p0$ | |
| $\langle ab\|u\|cd\rangle$ | 0.0635921 | −0.752945 | −0.705224 | −0.0452261 | |
| $bcd$ | $2s, 2p0, 2s$ | $2s, 2s, 2p0$ | $2p1, 2p0, 2p1$ | $2p1, 2p1, 2p0$ | |
| $\langle ab\|u\|cd\rangle$ | −0.838229 | −0.138923 | −0.756463 | −0.0185365 | |

TABLE IV. Theoretical values of the THFI parameters $A_s$ and $A_p$ (in MHz) for the first fluorine shell of $Yb^{3+}$ in $CsCaF_3$ and $Cs_2NaYF_6$ (see text for details).

| Crystal | Parameter | $A_d$ | $V_1$ | $V_2$ | $V_3$ | $V_4$ | $V_5$ | Sum | Expt. |
|---|---|---|---|---|---|---|---|---|---|
| $CsCaF_3$ | $A_s$ | 0 | 10.2 | 3.5 | 0.1 | 0 | 4 | 17.8 | 20.577 |
| $Cs_2NaYF_6$ | | | | | | 1.3 | | 19.1 | 22.111 |
| $CsCaF_3$ | $A_p$ | −9.0 | 2.5 | 0.8 | −0.3 | 0 | −0.2 | −6.2 | −5.963 |
| $Cs_2NaYF_6$ | | | | | | −0.5 | | −6.7 | −6.208 |

corrections to the transition amplitudes, the contributions of the above processes for other ions will be expressed through these functions as well.

$$f_{fi}^{(1)} = \frac{1}{4}q_{4fi}^2 - p_{4fi}\bar{\gamma}_{4fi} + \bar{\gamma}_{4fi}^2, \quad i = s,\sigma,\pi, \tag{9}$$

$$f_{f\sigma\pi}^{(1)} = \frac{1}{4}q_{4f\sigma}q_{4f\pi} - \frac{1}{2}p_{4f\sigma}\bar{\gamma}_{4f\pi} - \frac{1}{2}\bar{\gamma}_{4f\sigma}p_{4f\pi} + \bar{\gamma}_{4f\sigma}\bar{\gamma}_{4f\pi}. \tag{10}$$

Functions (9) and (10) refer to the $V_1$ operator,

$$f_{di}^{(2)} = \frac{h_{ri}}{|\Delta_{4f,i}|}\left[\frac{1}{4}p_{5di}p_{4fi} - \frac{1}{2}p_{5di}\bar{\gamma}_{4fi} + \frac{1}{2}\bar{\gamma}_{5di}p_{4fi} - \left(1 + \frac{|\Delta_{4fi}|}{|\Delta_{5di}|}\right)\bar{\gamma}_{5di}\bar{\gamma}_{4fi}\right], \tag{11}$$

where $\Delta_{4fs}=\Delta_{4f,2s}$, $\Delta_{4f\sigma}=\Delta_{4f\pi}=\Delta_{4f,2p}$ and for $\Delta_{5di}$ analogously; $h_i$ are the matrix elements of the $h_{eh}$ operator,

$$f_{d\sigma\pi}^{(2)} = \frac{1}{|\Delta_{4f,2p}|}\left[\frac{1}{4}(h_\sigma p_{5d\sigma}p_{4f\pi} + h_\pi p_{5d\pi}p_{4f\sigma}) - \frac{1}{2}(h_\sigma p_{5d\sigma}\bar{\gamma}_{4f\pi} + h_\pi p_{5d\pi}\bar{\gamma}_{4f\sigma}) + \frac{1}{2}(h_\sigma\bar{\gamma}_{5d\sigma}p_{4f\pi} + h_\pi\bar{\gamma}_{5d\pi}p_{4f\sigma}) - (h_\sigma\bar{\gamma}_{5d\sigma}\bar{\gamma}_{4f\pi} + h_\pi\bar{\gamma}_{5d\pi}\bar{\gamma}_{4f\sigma})\left(1 + \frac{|\Delta_{4f,2p}|}{|\Delta_{5d,2p}|}\right)\right]. \tag{12}$$

Functions (11) and (12) refer to the $V_2$ operator,

$$f_{f\sigma s}^{(4)} = \frac{h_{l\sigma s}}{|\Delta_{4fs}|}\left(\frac{1}{4}p_{4f\sigma}p_{4fs} - \frac{1}{2}p_{4f\sigma}\bar{\gamma}_{4fs} - \frac{1}{2}\bar{\gamma}_{4f\sigma}p_{4fs} + \bar{\gamma}_{4f\sigma}\bar{\gamma}_{4fs}\right), \tag{13}$$

where $h_{l\sigma s}$ is the matrix element of the $h_{eh}$ operator of the ligand. Function (13) refers to the $V_4$ operator.

The analytical expressions for the contributions of the $V_3$ operator to the THFI parameters for an octahedrally surrounded $Yb^{3+}$ ion are given in Ref. 17. To transfer to first-principles calculations from the semiempirical expressions in the present approach, it is necessary to perform the following substitution in formulas (12a) and (12b) of Ref. 17,

$$\lambda_{id}\gamma_{jd} \Rightarrow \bar{\gamma}_{5di}\bar{\gamma}_{5dj} - \frac{1}{4}p_{5di}p_{5dj}, \quad i,j = s,\sigma,\pi,$$

where $\lambda_{id}=s_{id}+\gamma_{id}$, $s_{id}$ is the overlap integral, and $\gamma_{id}$ is a fitting parameter.[17] We denote these contributions as $T_\parallel^{(3)}$ and $T_\perp^{(3)}$.

The transition from the second-quantization operators $V_i$ to the spin Hamiltonian is performed in a standard way[17] and for the contributions to the THFI parameters we obtain

$$T_\parallel = \frac{1}{3}(f_{fs}^{(1)} + 2f_{ds}^{(2)} + 2f_{f\sigma s}^{(4)})a_s + \left(\frac{2}{3}(f_{f\sigma}^{(1)} + 2f_{d\sigma}^{(2)}) + \frac{3}{2}(f_{f\pi}^{(1)} + 2f_{d\pi}^{(2)}) - \sqrt{\frac{3}{2}}(f_{f\sigma\pi}^{(1)} + f_{f\sigma\pi}^{(2)})\right)a_p + T_\parallel^{(3)}$$

$$T_\perp = -\frac{1}{3}(f_{fs}^{(1)} + 2f_{ds}^{(2)} + 2f_{f\sigma s}^{(4)})a_s + \left(\frac{1}{3}(f_{f\sigma}^{(1)} + 2f_{d\sigma}^{(2)}) + \frac{3}{4}(f_{f\pi}^{(1)} + 2f_{d\pi}^{(2)}) - \frac{13}{6}\sqrt{\frac{3}{2}}(f_{f\sigma\pi}^{(1)} + f_{d\sigma\pi}^{(2)})\right)a_p + T_\perp^{(3)},$$

where $a_s$ and $a_p$ are the parameters of the THFI of the fluorine free ion [$a_s=45.06\times10^3$ MHz and $a_p=1.29\times10^3$ MHz (Ref. 1)].

According to Ref. 18, the matrix elements of the $h_{eh}$ operator are

$$\langle 5d0|h_{eh}|4f0\rangle = h_s = h_\sigma = 0.0355,$$
$$\langle 5d1|h_{eh}|4f1\rangle = h_\pi = 0.0335.$$

The matrix elements of $h_{eh}$ according to Ref. 40 in the first approximation are determined by the electron-hole Coulomb interaction. In this approximation, the calculation on the wave functions[37] results in $\langle 2p0|h_{eh}|2s\rangle = h_{l\sigma s} = -0.036$. According to Ref. 18, $\Delta_{5d,2s}\approx 1.5$ a.u. and $\Delta_{5d,2p}\approx 0.68$ a.u. The calculated values of $q_{\xi\theta}$ and $p_{\xi\theta}$, necessary to perform estimates, are given below,

$$q_{4fs} = -0.009\,290\,64, \quad q_{4f\sigma} = -0.013\,98,$$
$$q_{4f\pi} = 0.008\,382\,87,$$

$$p_{4fs} = 0.009\,665\,65, \quad p_{4f\sigma} = 0.014\,604\,5,$$
$$p_{4f\pi} = -0.008\,624\,18,$$

$$p_{5ds} = -0.2303, \quad p_{5d\sigma} = -0.2105, \quad p_{5d\pi} = 0.1292.$$

By substituting these and above values in formulas (9)–(13) we obtain the values of the $A_f$ and $A_p$ parameters

given in Table IV, which also shows the terms corresponding to the contributions of the $V_1$, $V_2$, $V_3$, and $V_4$ parameters. As indicated above, the contributions of the $V_5$ operator are estimated using the approach of Ref. 19. Table IV shows that the given approach allowed us to obtain both the correct order of magnitude and sign of the experimental THFI values and to explain the origin of their difference observed for very similar structures. The above analysis shows that all processes considered here should be taken into account when interpreting the spectroscopic data of rare-earth impurity centers.

## V. CONCLUSIONS

The results of the present work allow us to conclude that the developed second-quantization method within the framework of virtual and real processes of charge transfer from a ligand to a metal ion enables one to obtain mathematically correct expressions for calculating the contributions of these processes to the physical parameters of the impurity center, as well as for calculating the transition amplitudes from first principles. It is shown that these processes are to be taken into account in the interpretation of experimental THFI data of RE impurities. It should be noted that the expressions for the operators of the considered one-particle processes are not only applicable to THFI of the complete RE series but also for impurity centers of other transition elements; i.e., they are of general character. Moreover, these processes should be taken into account when calculating other properties of the impurity ion, i.e., its self-hyperfine interaction, crystal field parameters, oscillator strengths of optical transitions, etc.

Experiment and calculations show that the appearance of the hyperfine fields on the ligand nuclei is mainly determined by the processes within the first coordination sphere. From a quantitative point of view, the following refinements of the calculations could still be considered. First, the contributions of core polarization within the proposed approaches could be calculated from first principles. Second, the influence of the $R_{\text{Yb-F}}$ distance on the calculated THFI parameters should be further studied since this is the only (theoretical) input parameter in the model. One cannot exclude some influence of the next coordination spheres surrounding the RE ion, i.e., via their inclusion in the $(I+S)^{-1}$ matrix. The success in explaining the differences in THFI parameters, however, gives us hope that also the optical data obtained in Ref. 24 will be explained using the approach considered here.

## ACKNOWLEDGMENTS

This work was supported by the Russian Foundation for Basic Research (Project No. 06-02-17481) and by the Flemish Research Foundation (FWO). One of the authors (M.L.F.) gratefully acknowledges the Deutscher Akademischer Austauschdienst (DAAD) grant. H.V. acknowledges support of FWO. The authors are grateful to R.Yu. Abdulsabirov and S.L. Korableva for crystal growth ($CsCaF_3:Yb^{3+}$).

[1] S. Sugano and R. G. Shulman, Phys. Rev. **130**, 517 (1963).
[2] A. J. H. Wachters and W. C. Nieuwport, Phys. Rev. B **5**, 4291 (1972).
[3] J. Hubbard, D. E. Rimmer, and F. R. A. Hopgood, Proc. Phys. Soc. London **88**, 13 (1966).
[4] Y. Shen and K. L. Bray, Phys. Rev. B **58**, 5305 (1998).
[5] B. R. McGarvey, J. Chem. Phys. **65**, 955 (1976).
[6] B. Z. Malkin, in *Spectroscopy of Solids Containing Rare-Earth Ions*, edited by A. A. Kaplyanskii and R. M. Macfarlane (North-Holland, Amsterdam, 1987), p. 13.
[7] B. Z. Malkin, A. M. Leushin, A. I. Iskhakova, J. Heber, M. Altwein, K. Moller, I. I. Faslizhanov, and V. A. Ulanov, Phys. Rev. B **62**, 7063 (2000).
[8] P. Hohenberg and W. Kohn, Phys. Rev. **136**, B864 (1964).
[9] W. Kohn and L. J. Sham, Phys. Rev. **140**, A1133 (1965).
[10] J. M. Garcia-Lastra, T. A. Wesolowski, M. T. Barriuso, J. A. Aramburu, and M. Moreno, J. Phys.: Condens. Matter **18**, 1519 (2006).
[11] P. Husser, H. U. Suter, E. P. Stoll, and P. F. Meier, Phys. Rev. B **61**, 1567 (2000).
[12] M. Moshinsky and T. H. Seligman, Ann. Phys. (N.Y.) **66**, 311 (1971).
[13] E. Artacho and L. M. Bosch, Phys. Rev. A **43**, 5770 (1991).
[14] M. V. Eremin and A. M. Leushin, Phys. Solid State **16**, 1917 (1974).
[15] M. V. Eremin and A. A. Kornienko, Phys. Solid State **19**, 3024 (1977).
[16] B. R. Judd, *Second Quantization and Atomic Spectroscopy* (The Johns Hopkins Press, Baltimore, 1967), p. 210.
[17] O. A. Anikeenok, M. V. Eremin, M. L. Falin, and V. P. Meiklyar, J. Phys. C **15**, 1557 (1982).
[18] O. A. Anikeenok, M. V. Eremin, M. L. Falin, A. L. Konkin, and V. P. Meiklyar, J. Phys. C **17**, 2813 (1984).
[19] M. L. Falin, M. V. Eremin, H. Bill, and D. Lovy, Appl. Magn. Reson. **9**, 329 (1995).
[20] O. A. Anikeenok, Phys. Solid State **45**, 854 (2003).
[21] O. A. Anikeenok, Phys. Solid State **47**, 1100 (2005).
[22] R. W. G. Wyckoff, *Crystal Structure*, 2nd ed. (Interscience, New York, 1964), Vol. 2, p. 588.
[23] G. Meyer, Prog. Solid State Chem. **14**, 141 (1982).
[24] M. L. Falin, K. I. Gerasimov, A. M. Leushin, and N. M. Khaidukov, J. Lumin. **128**, 1103 (2008).
[25] Th. Pawlik, J.-M. Spaeth, M. Otte, and H. Overhof, Radiat. Eff. Defects Solids **135**, 49 (1995).
[26] M. L. Falin, V. P. Meiklyar, and A. L. Konkin, J. Phys. C **13**, 1299 (1980).
[27] V. A. Latypov and M. L. Falin, Prib. Tekh. Eksp. **4**, 164 (2001).
[28] A. Abragam and B. Bleaney, *Electron Paramagnetic Resonance of Transition Ions* (Oxford University Press, Oxford, 1970), p. 700.
[29] M. M. Zaripov, V. P. Meyklyar, and M. L. Falin, Pis'ma Zh. Eksp. Teor. Fiz. **29**, 265 (1979) [JETP Lett. **29**, 237 (1979)].
[30] V. F. Bespalov, M. L. Falin, B. N. Kazakov, A. M. Leushin, I. R. Ibragimov, and G. M. Safiullin, Appl. Magn. Reson. **11**, 125

(1996).
[31] A. P. Prudnikov, Yu. A. Brychkov, and O. I. Marichev, *Integraly I ryady* (Nauka, Moscow, 1981) (in russian).
[32] G. L. Bir and G. E. Pikus, *Symmetry and Strain-Induced Effects in Semiconductors* (Nauka, Moscow, 1972); *ibid.* (Wiley, New York, 1975).
[33] O. A. Anikeenok, Phys. Solid State **48**, 1878 (2006).
[34] W. H. Adams, J. Chem. Phys. **34**, 89 (1961).
[35] A. B. Kunz, Phys. Rev. B **4**, 609 (1971).
[36] R. D. Shannon, Acta Crystallogr., Sect. A: Found. Crystallogr. **32**, 751 (1976).
[37] E. Clementi and L. Roetti, At. Data Nucl. Data Tables **14**, 177 (1974).
[38] K. Rajnak, J. Chem. Phys. **37**, 2440 (1962).
[39] N. L. Huang, R. Orbach, E. Simanek, J. Owen, and D. R. Taylor, Phys. Rev. **156**, 383 (1967).
[40] O. Madelung, *Festkörpertheorie II* (Springer-Verlag, Berlin, 1972), p. 203.